Supporting Information

Nano-engineering induced Bi dots *in-situ* anchored into modified porous carbon with superior sodium ion storage

Jun Chen,[a] Jun Xiao,[a,b] Jiayi Li,[a] Hong Gao,*[a,b] Xin Guo,[b] Hao Liu,*[a,b] and Guoxiu Wang*[b]

[a] International Laboratory on Environmental and Energy Frontier Materials, School of Environmental and Chemical Engineering, Shanghai University, Shanghai 200444, P. R. China.
E-mail: Candy1122@shu.edu.cn

[b] Centre for Clean Energy Technology, Faculty of Science, University of Technology Sydney, Broadway, Sydney, NSW 2007, Australia.
E-mail: hao.liu@uts.edu.au, Guoxiu.Wang@uts.edu.au

Detailed steps for in situ XRD testing:

The Bi@MC slurry was pasted onto an aluminum net, followed by drying at 120°C under vacuum for 12 h. The dried material was used as the electrode. Sodium foil and glass fiber was severed as the counter electrode and separator, respectively, and 1.0 M $NaPF_6$ in DME as electrolyte. The XRD chamber was equipped with a Be window to permit X-ray passage. *In situ* XRD patterns of the Bi@MC electrodes were tested on Bruker D8 Advanced (Cu Kα) and studied by a specially-made chamber (Beijing scistar technology co. ltd) in a scanning range of 10-90°(2θ) with step increment of 2.5°. The Be foil is the X-ray penetrator. The corresponding galvanostatic charge-discharge cycling was carried out at a current density of 100 mA g^{-1} between 0.1 and 1.6 V versus Na^+/Na.

The Bi content was calculated based on the following equation:

$$Bi(wt\%) = \frac{final\ weight\ of\ Bi_2O_3}{initial\ weight\ of\ Bi@MC} \times \frac{2 * molecular\ weight\ of\ Bi}{molecular\ weight\ of\ Bi_2O_3} \times 100\%$$

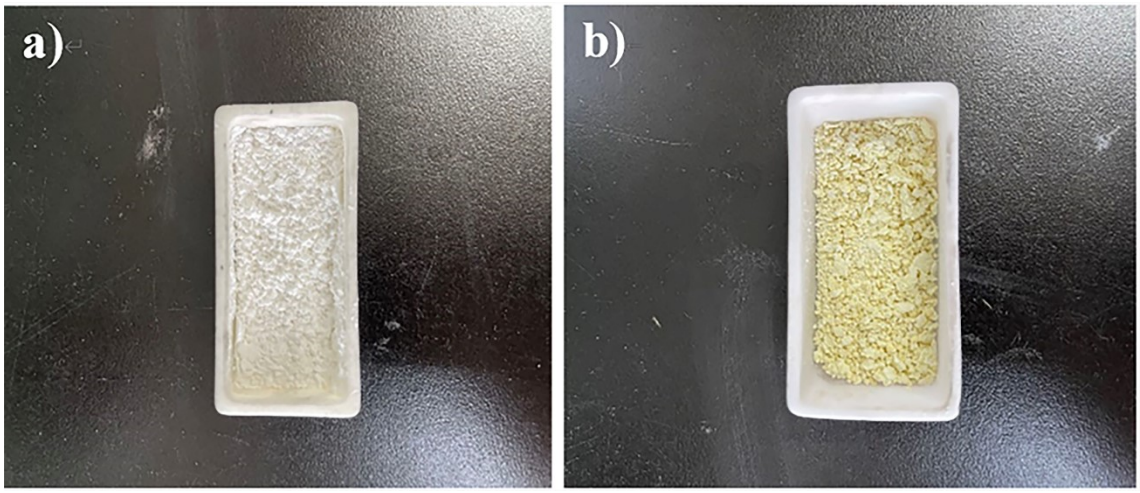

Fig. S1 Digital photographs of a) bismuth subsalicylate (BS) and b) a mixture of BS and KOH.

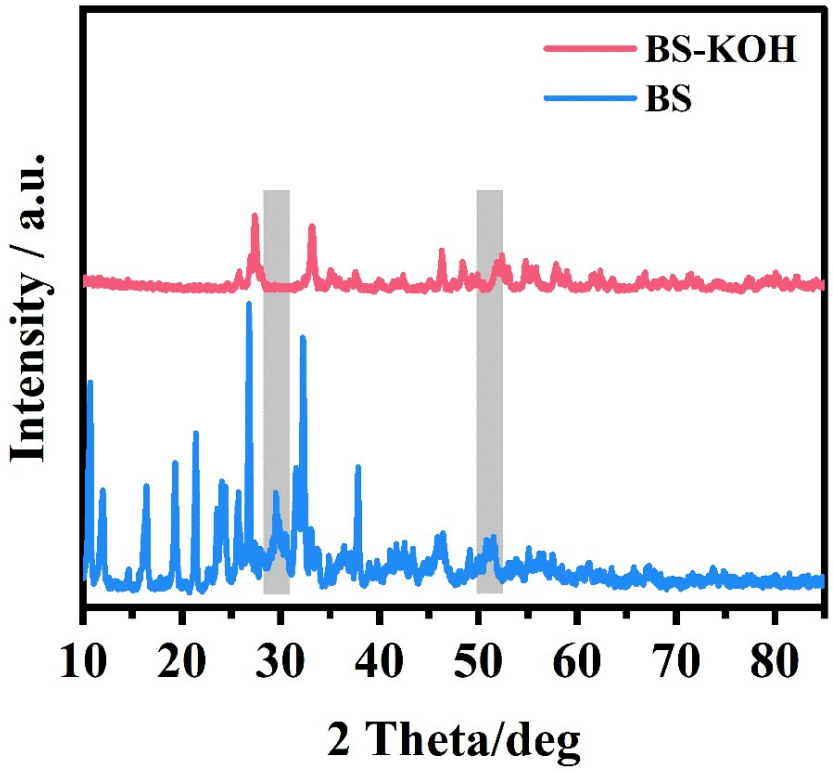

Fig. S2 XRD patterns of BS and the mixture of BS and KOH.

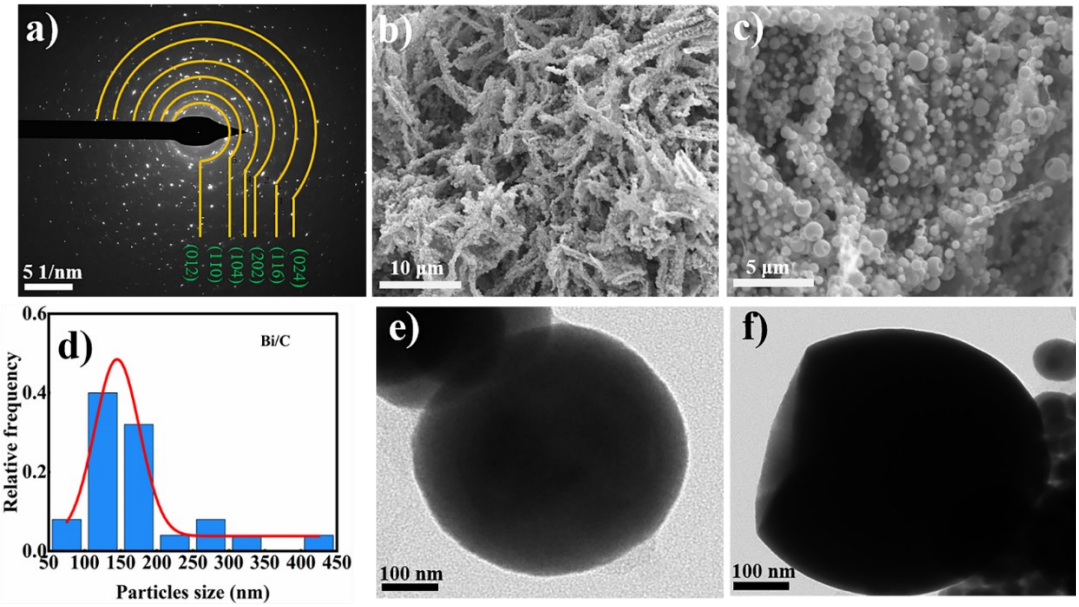

Fig. S3 a) SAED image of Bi@MC, b-c) SEM images of Bi/C, d) the size distribution of Bi/C, e-f) TEM images of Bi/C.

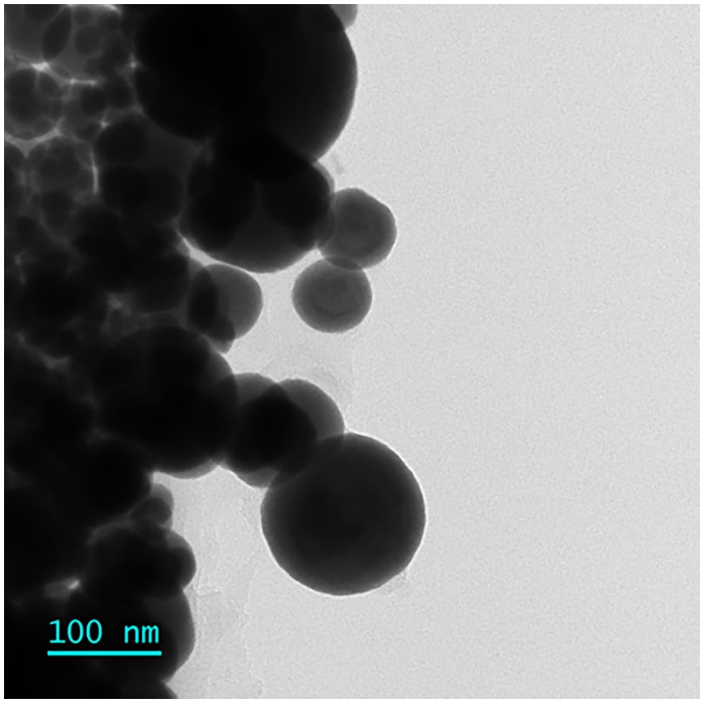

Fig. S4 TEM image was used to calculate the particle size distribution of Bi/C.

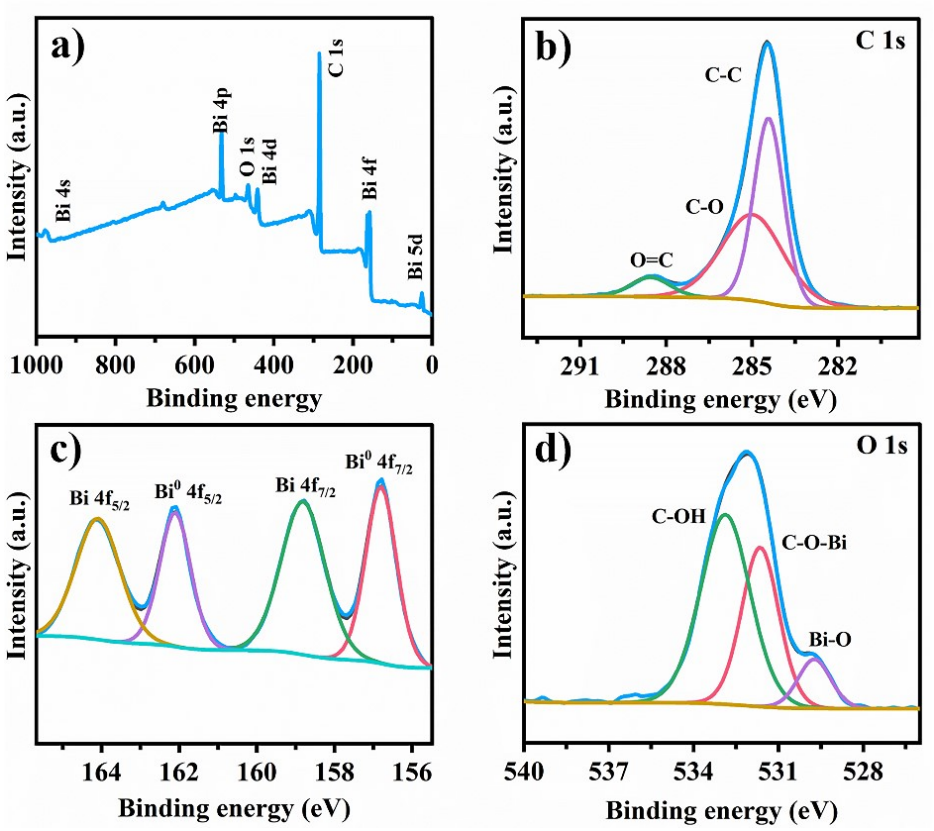

Fig. S5 XPS spectra of (a) full survey, (b) high-resolution C 1s, (c) high-resolution Bi 4f, and (d) high-resolution O1s for Bi/C.

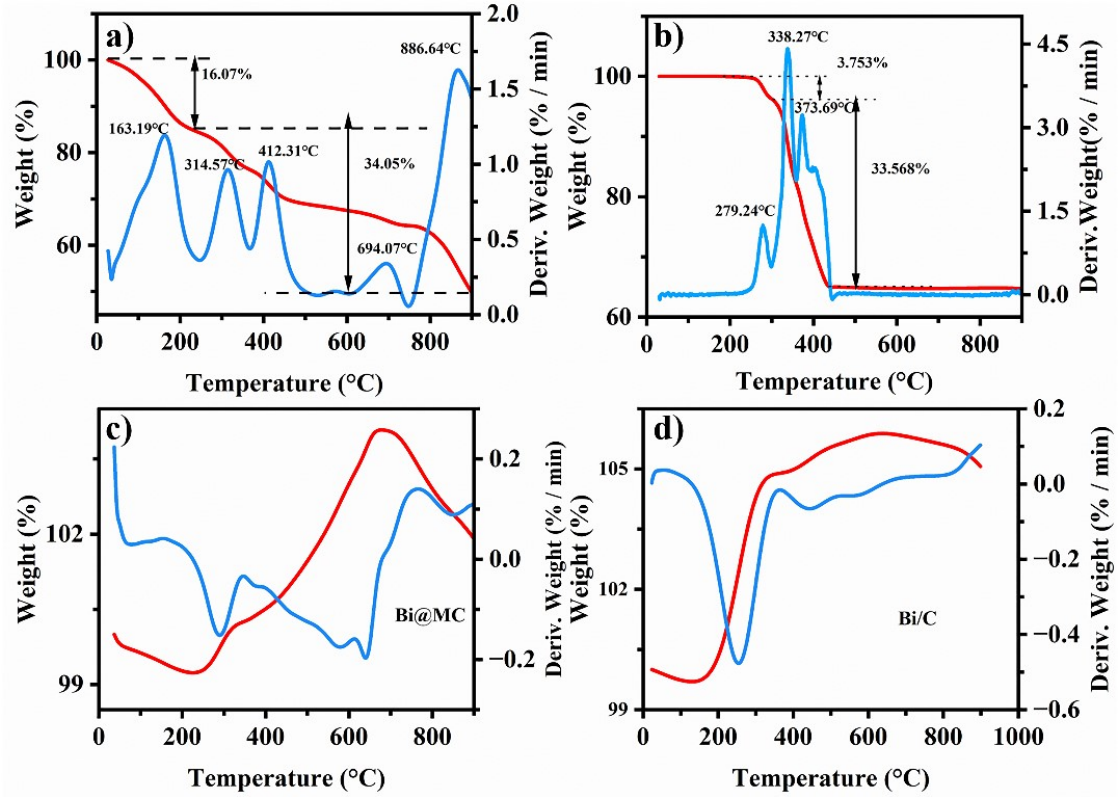

Fig. S6 The TGA curves of a) mixture of BS and KOH, b) BS in Ar, c) Bi@MC and d) Bi/C in air.

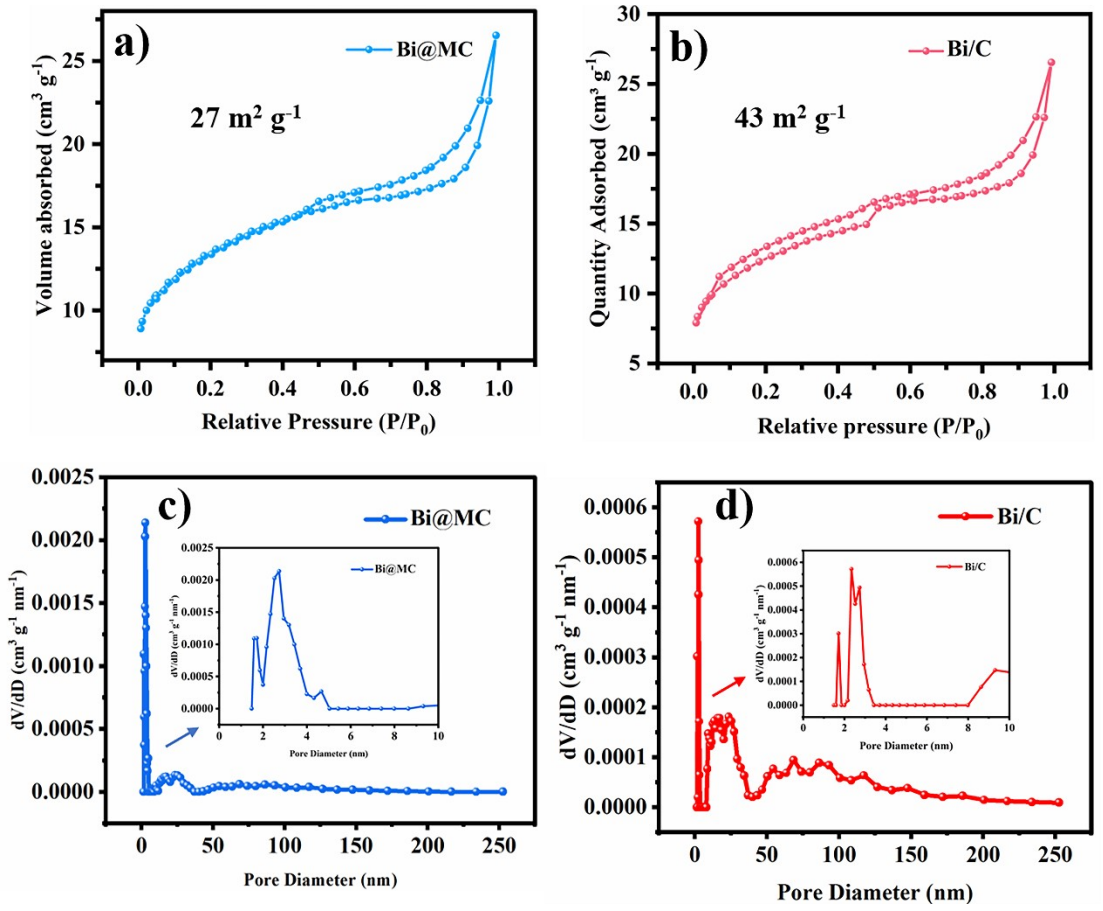

Fig. S7 N_2 adsorption-desorption isotherms spectra of a) Bi@MC and b) Bi/C. The pore size distribution of c) Bi@MC and d) Bi/C.

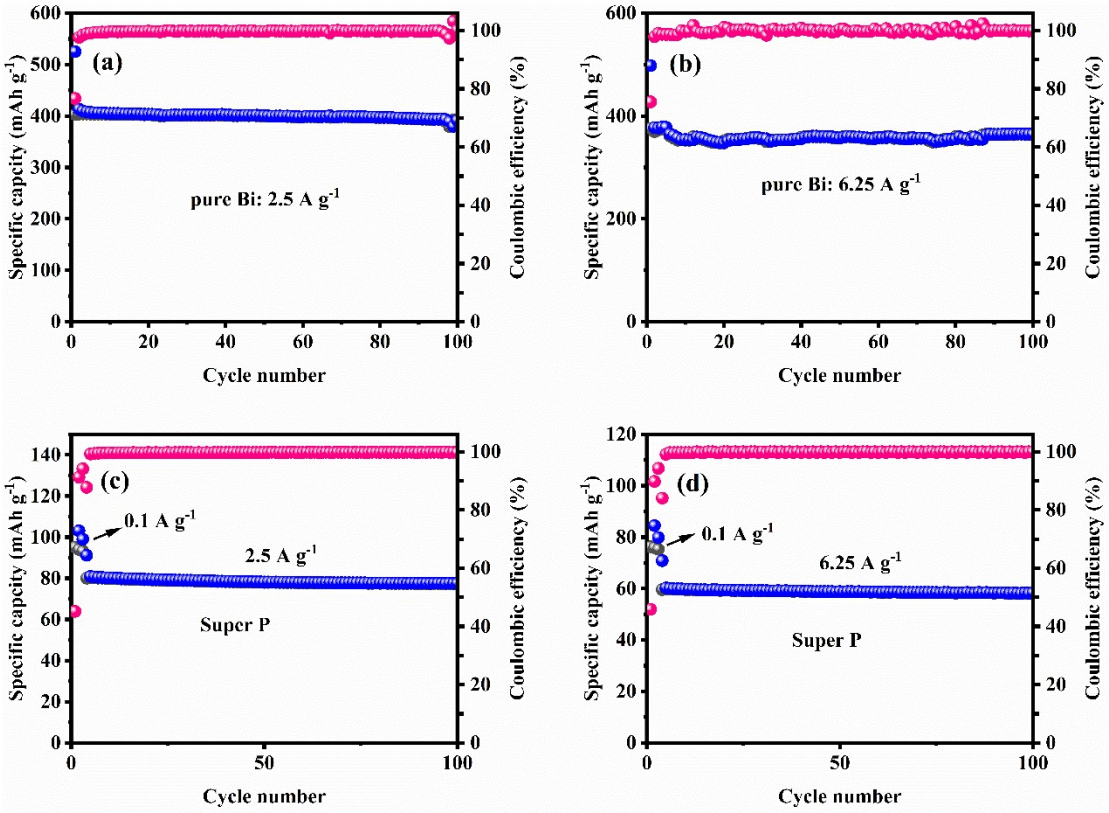

Fig. S8 Cycle performance of pure Bi and super P at a, c) 2.5 A g^{-1}, b, d) 6.25 A g^{-1}.

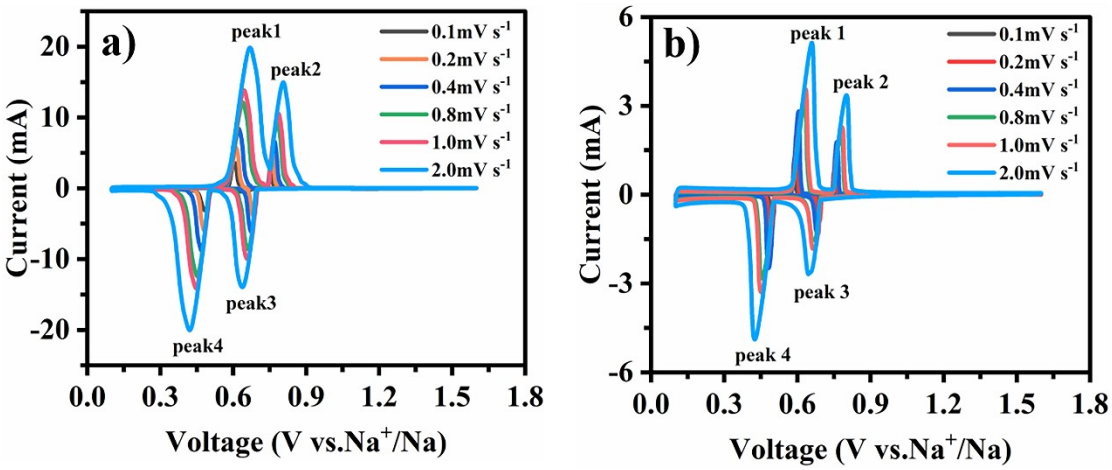

Fig. S9 CV curves of a) Bi@MC and b) Bi/C at different scan rates (0.1, 0.2, 0.4, 0.8, 1, and 2 mV s^{-1}, respectively).

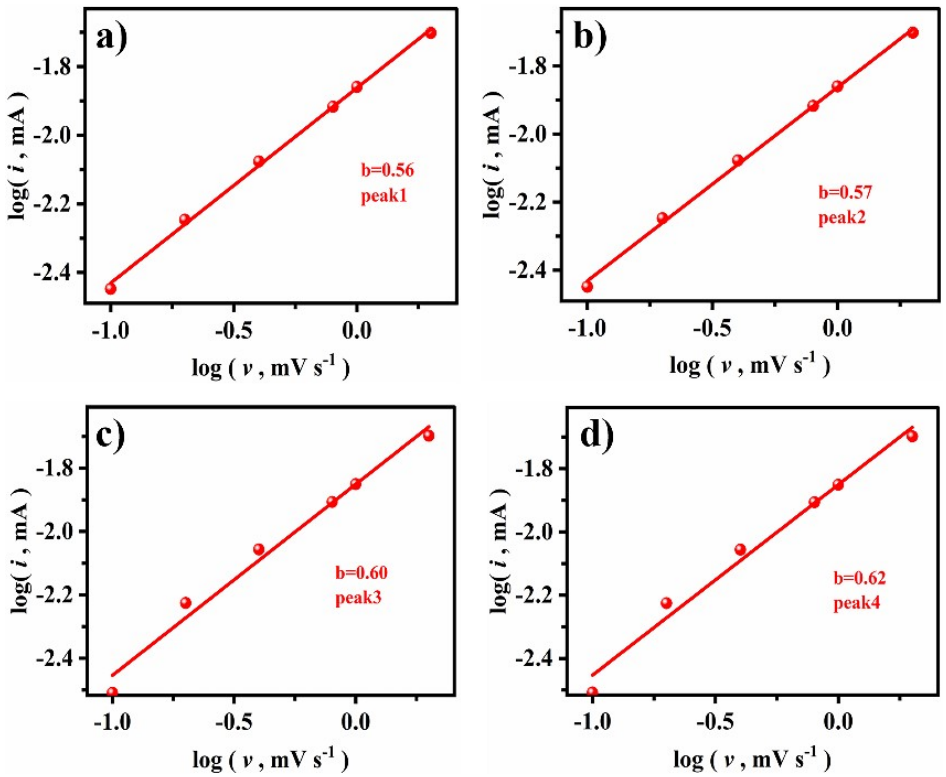

Fig. S10 The fitted linear relationship of log(*v*) versus log(*i*) for Bi/C based on the CV curves at different rates shown in Fig S8 b): a) peak1, b) peak2, c) peak3, d) peak4.

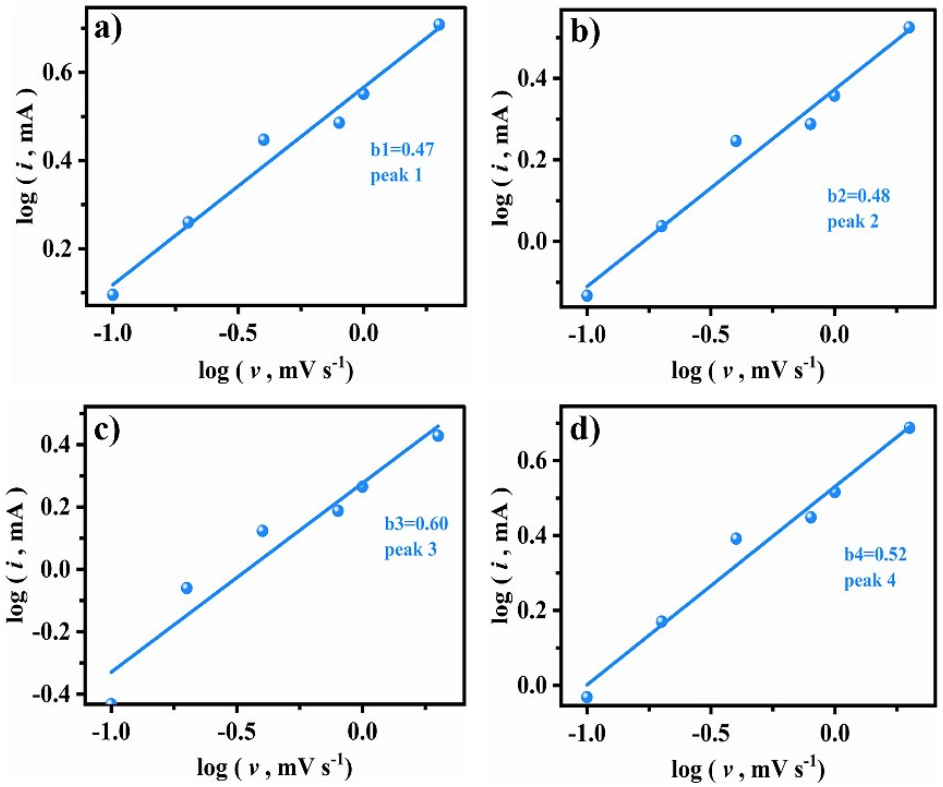

Fig. S11 The fitted linear relationship of log(v) versus log(i) for Bi@MC based on the CV curves at different rates shown in Fig S8 a): a) peak1, b) peak2, c) peak3, d) peak4.

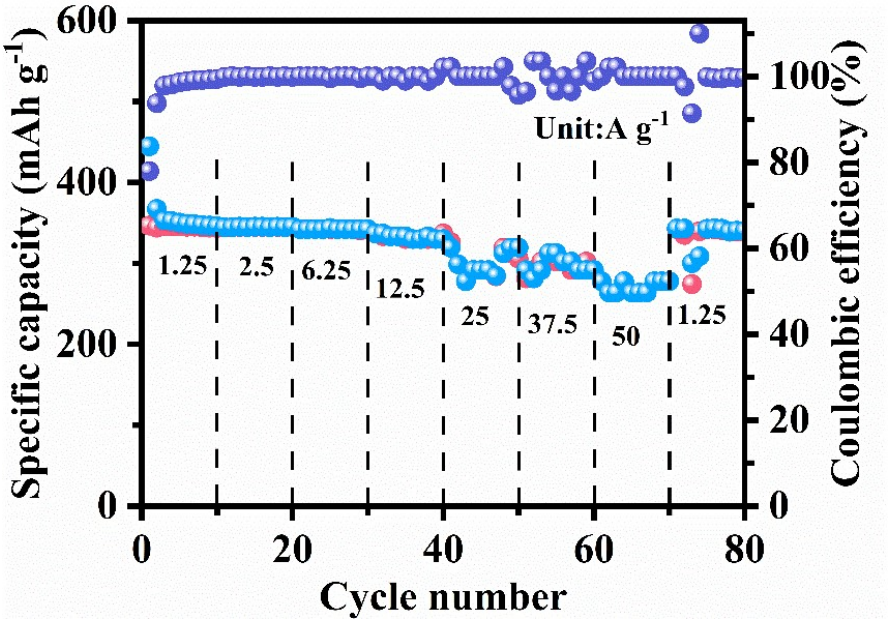

Fig. S12 Rate performance of the Bi/C electrode.

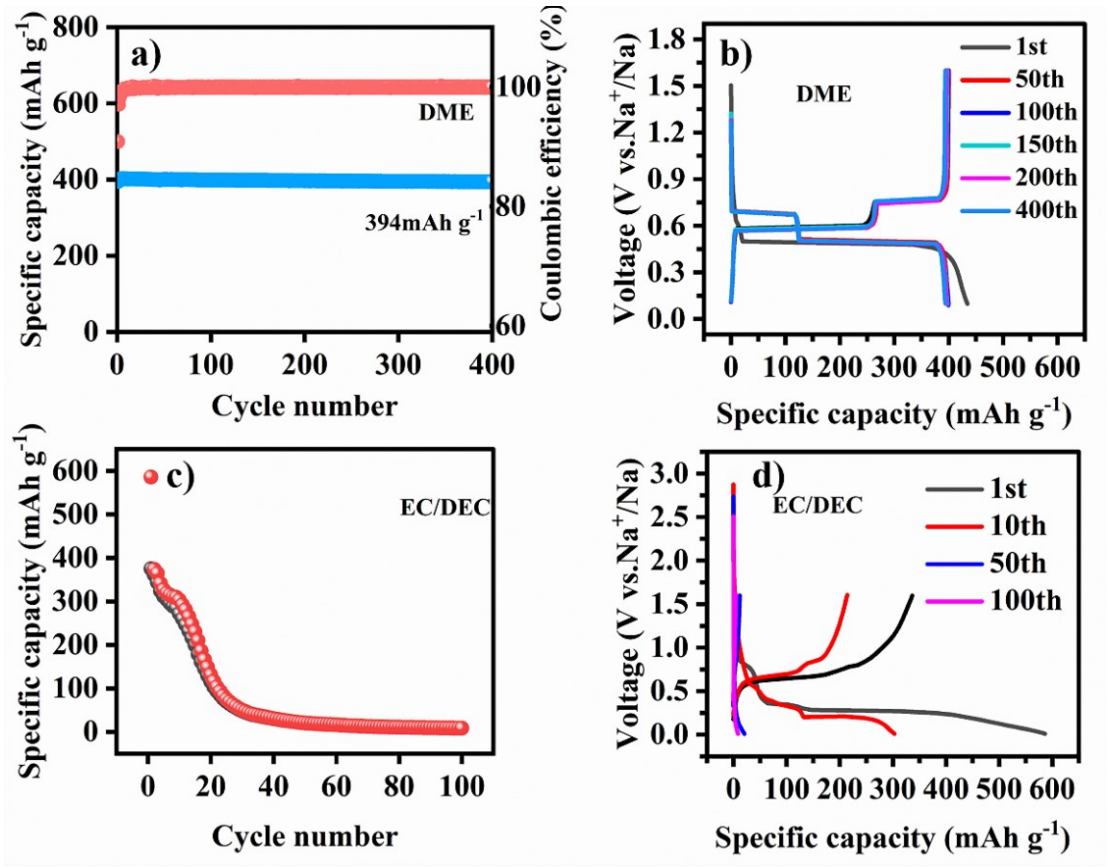

Fig. S13 a) Electrochemical performance and b) selected charge/discharge curves of Bi@MC in DME-based electrolyte at a current density of 1.25 A g^{-1}, c) electrochemical performance and d) selected charge/discharge curves of Bi@MC in EC/DEC-based electrolyte at a current density of 1.25 A g^{-1}.

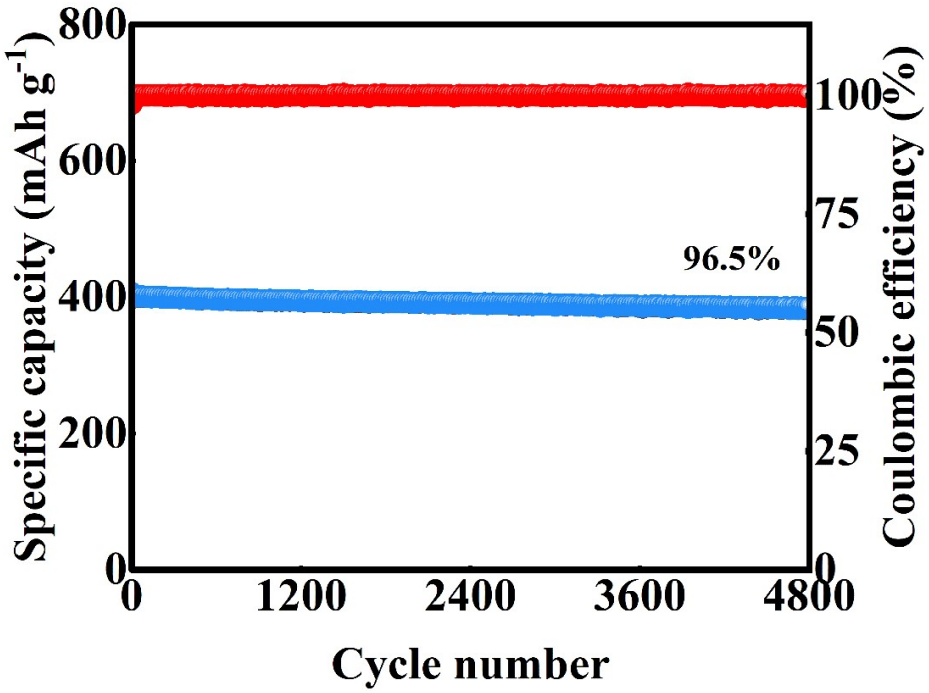

Fig. S14 Long cycle test of Bi@MC electrode at 5 A g^{-1}.

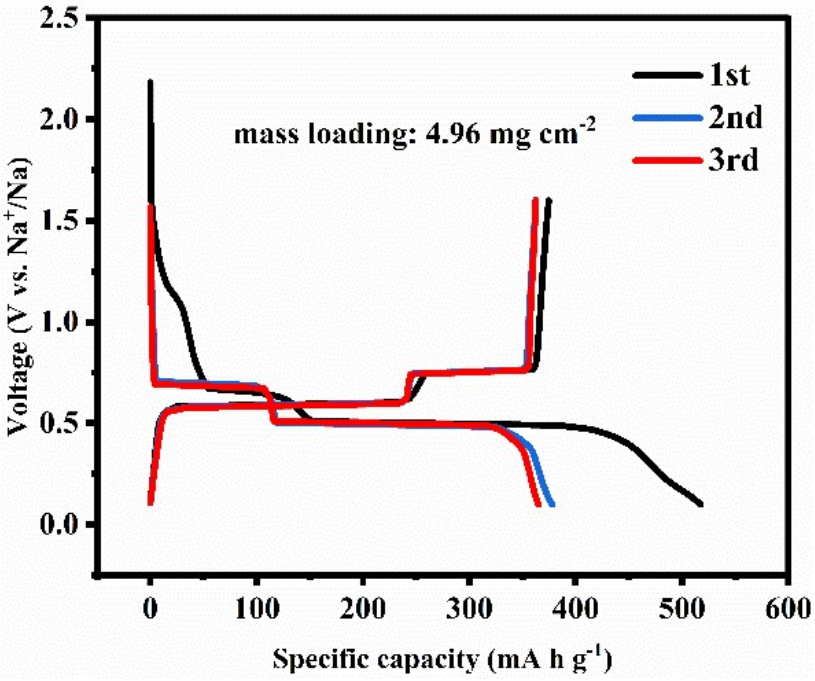

Fig. S15 The electrochemical performance of Bi@MC with mass loading of 4.96 mg cm^{-2}.

Table S1. Electrochemical comparison of this work with other reported Bi-based anodes for SIBs.

Electrode materials	**Capacity @ cycle number at current density**	**Rate performance (mAh g^{-1})**	**Reference**
Bi@MC	**378 mAh g^{-1}@ 10000 at 2.5 A g^{-1} 379 mAh g^{-1}@ 5000 at 6.25 A g^{-1}**	**345 mAh g^{-1}at 50000mA g^{-1}**	**This Work**
Bi@C⊂CFs	305 @ 5000 at 5 A g^{-1}	308.8 at 80000 mA g^{-1}	1
Bulk Bi	360 @ 3500 at 7.7 A g^{-1}	325 at 57750 mA g^{-1}	2
H-BiS/EGF	261@17300 at 5 A g^{-1}	228 at 25000 mA g^{-1}	3
HBiC	264@15000 at 5 A g^{-1}	297 at 10000 mA g^{-1}	4
Bi@graphene	200@50 at 40 mA g^{-1}	250 @1280 mA g^{-1}	5
Bi@C	300@100 at 150 mA g^{-1}	——	6
Bi@C microsphere	123.5@100 at 100 mA g^{-1}	83.4 @2000 mA g^{-1}	7
Bi nanorod bundle	301.9@150 at 50 mA g^{-1}	102.3@2000 mA g^{-1}	8
Bulk Bi	389@2000 at 400 mA g^{-1}	355@2000 mA g^{-1}	9
Bi-NS@C	106@1000 at 200 mA g^{-1}	110@2000 mA g^{-1}	10
Bi/CFC	350@300 at 50 mA g^{-1}	120@2000 mA g^{-1}	11
Bi/C nanofibers	273.2@500 at 100 mA g^{-1}	69@3200 mA g^{-1}	12
Bi nanoflakes	302.4@100 at 200 mA g^{-1}	206.4@2000 mA g^{-1}	13
Bi@graphite	~140@10000 at 3.2A g^{-1}	113@48000 mA g^{-1}	14
Bi@C nanoplates	200@200 at 150 mA g^{-1}	74@2000 mA g^{-1}	15
Bi@N-C	235@2000 at 10 A g^{-1}	178@100000 mA g^{-1}	16
Bi@3DGF	185.2@2000 at 10 A g^{-1}	194@50000 mA g^{-1}	17
Bi@N−C	302@1000 at 1 A g^{-1}	368@2000 mA g^{-1}	18

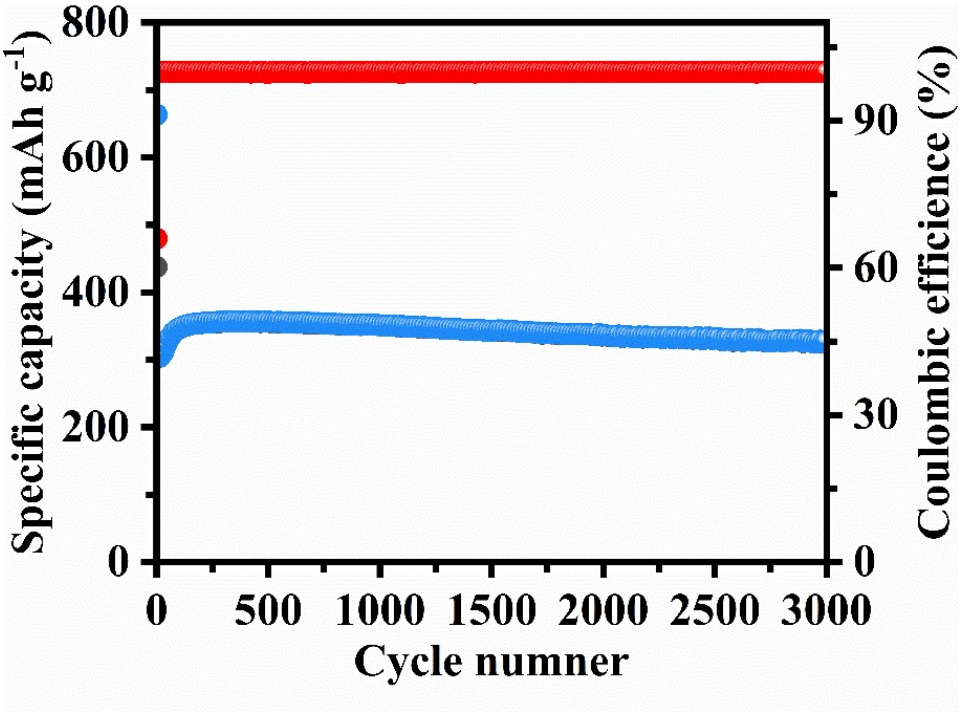

Fig. S16 Cycling performance of Bi/C electrode at a current density of 1.25 A g^{-1} after 3000 cycles.

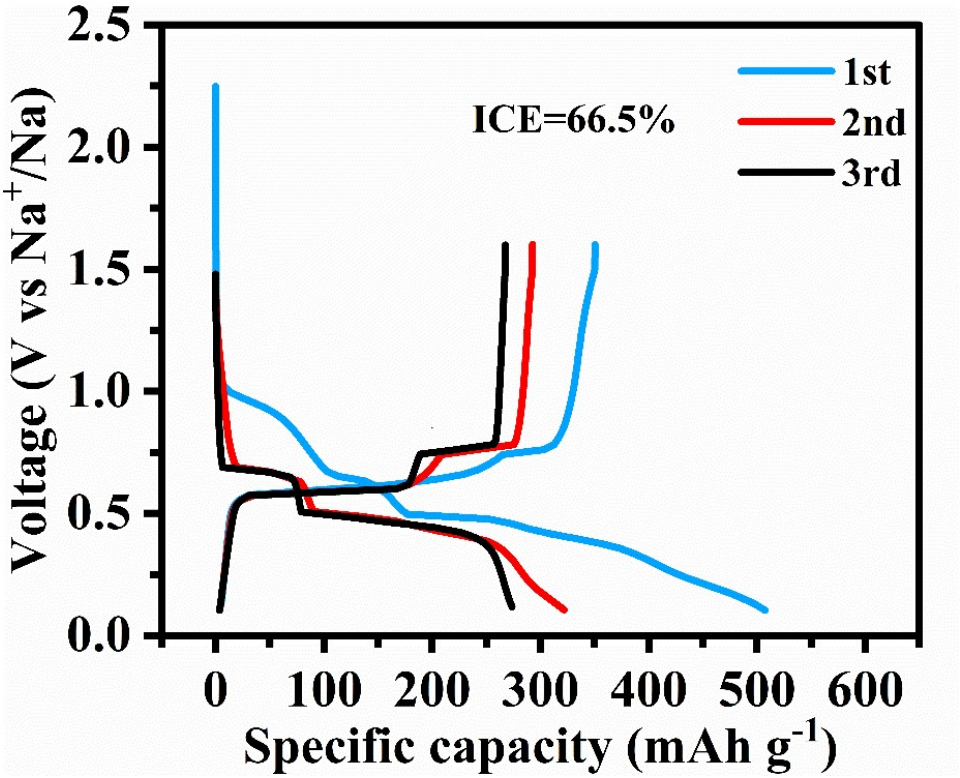

Fig. S17 First three charge/discharge curves of Bi/C electrode.

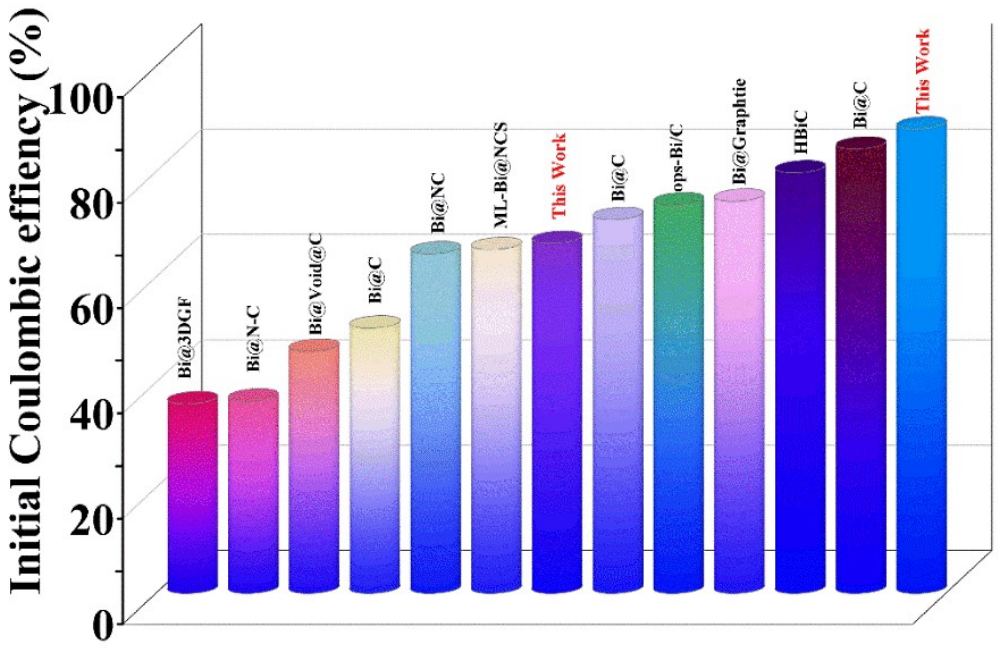

Fig.S18 Initial Coulombic efficiency comparison of this work with other reported Bi-based anodes for SIBs.

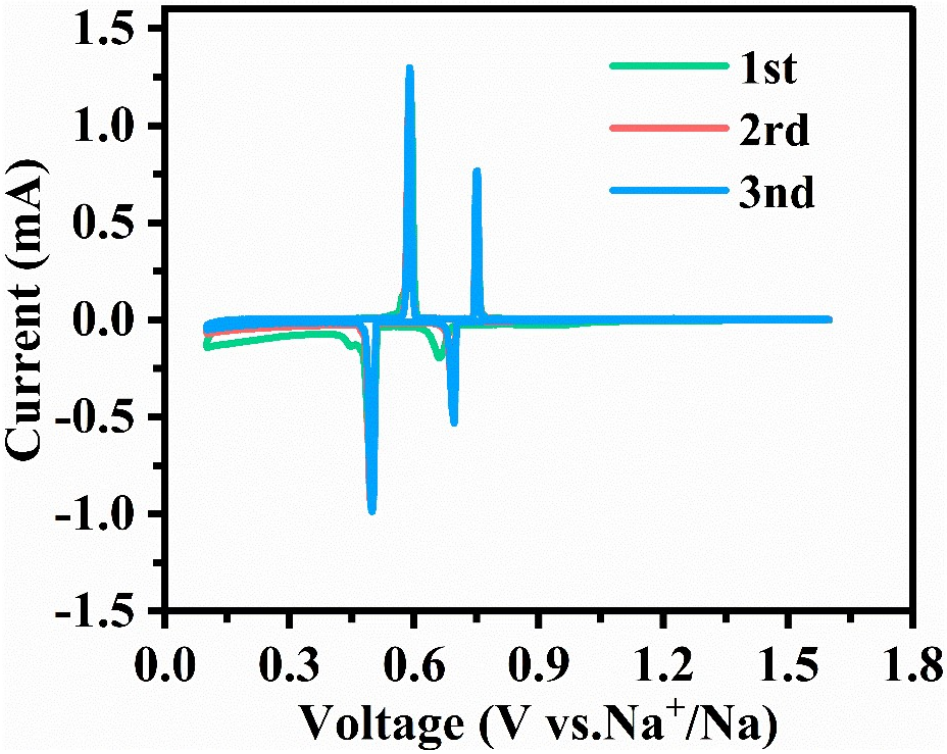

Fig.S19 First three CV curves of Bi/C electrode.

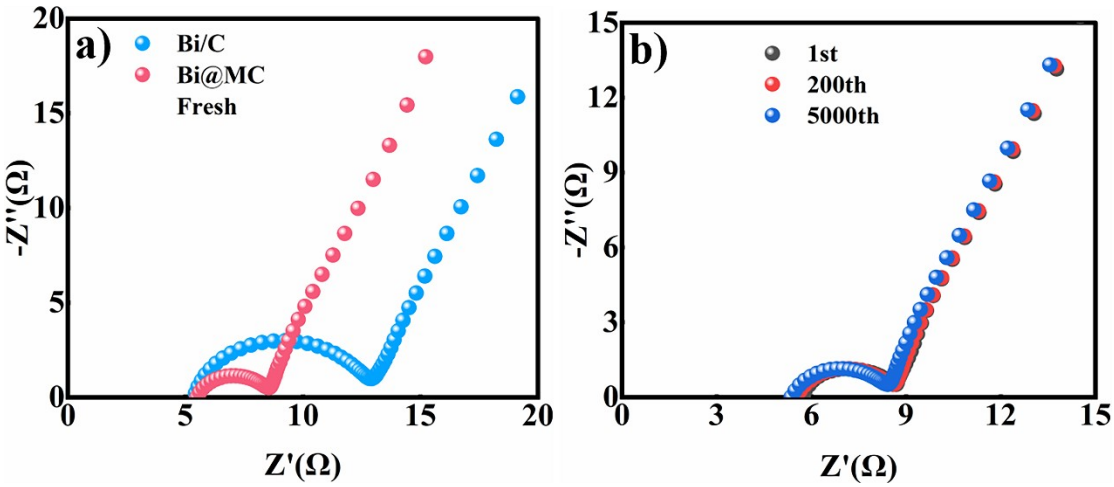

Fig. S20 a) Nyquist plots of fresh Bi@MC and Bi/C composite electrodes, b) Nyquist plots of Bi@MC electrode at 1st, 200th and 5000th cycle, respectively.

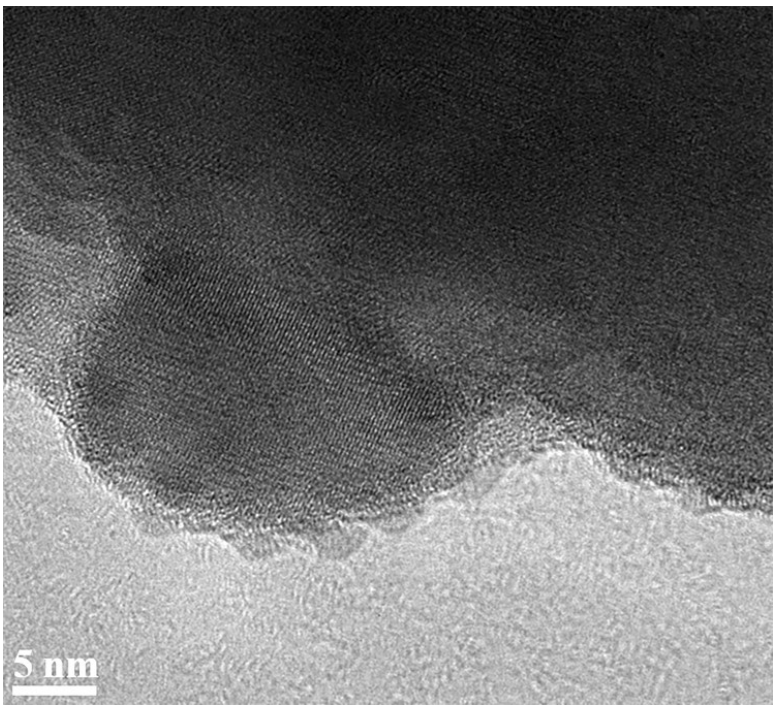

Fig. S21 the overview image of Fig. 4f.

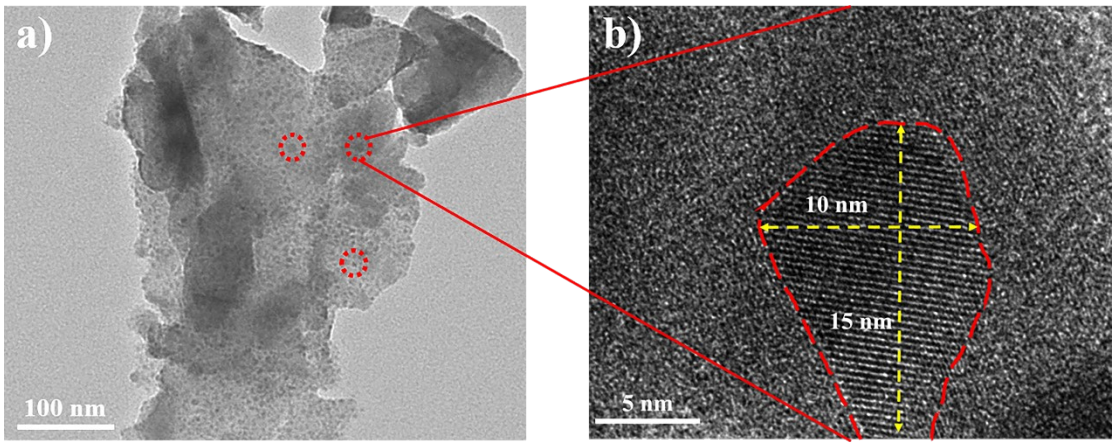

Fig. S22 HRTEM image of the Bi@MC electrode after 200 cycles.

Table S2. The distribution of two types oxygen-functional groups on Bi@MC and Bi/C composites.

Samples	O/C	C-OH (%)
Bi@MC	0.187	18.02
Bi/C	0.135	13.1

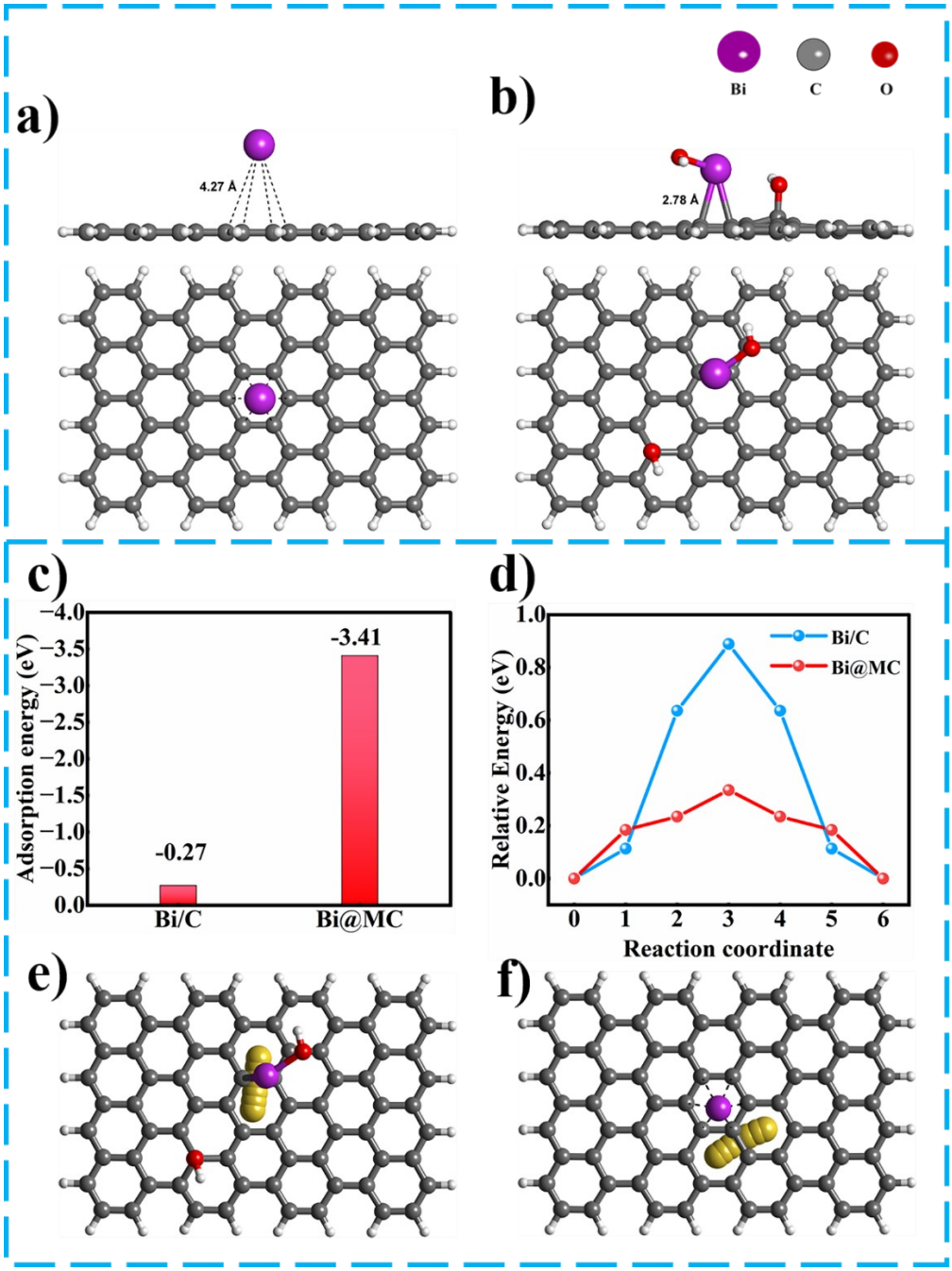

Fig. S23 Optimized structures of Bi adsorption on (a) graphene and (b) KOH-modified graphene. c) The calculated adsorption energy of Bi and d) Na diffusion energy barrier on graphene and KOH-modified graphene, respectively. Schematic representation of Na^+ diffusion path on (e) Bi-graphene and (f) Bi-graphene-KOH.

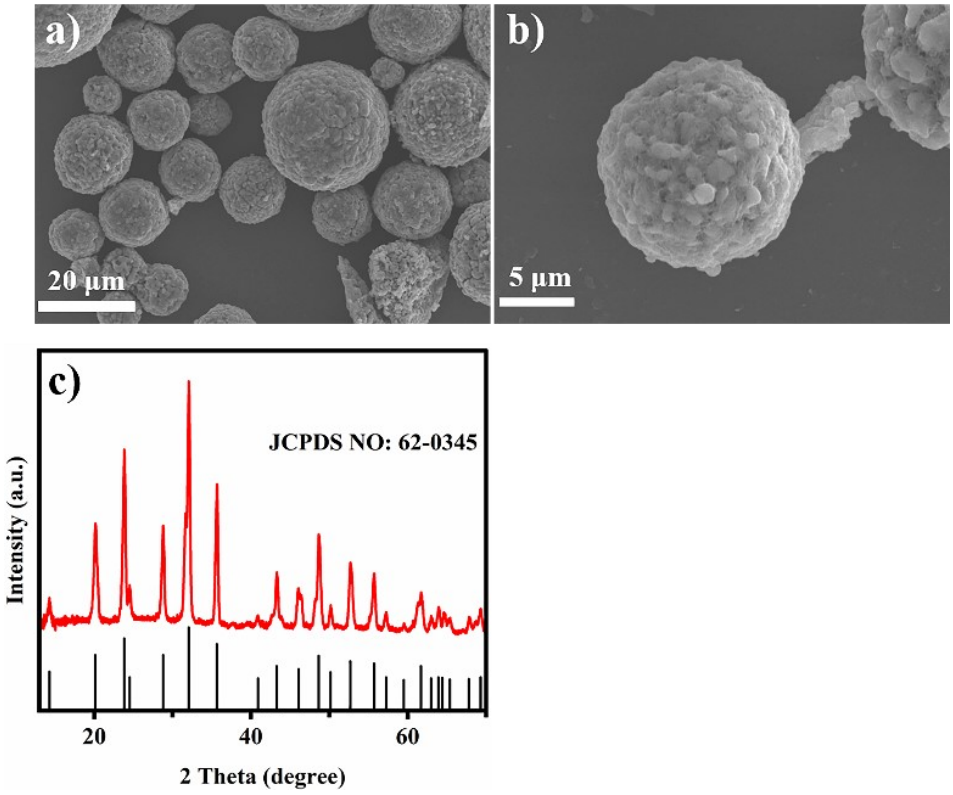

Fig. S24 The a, b) SEM image and c) XRD pattern of NVP.

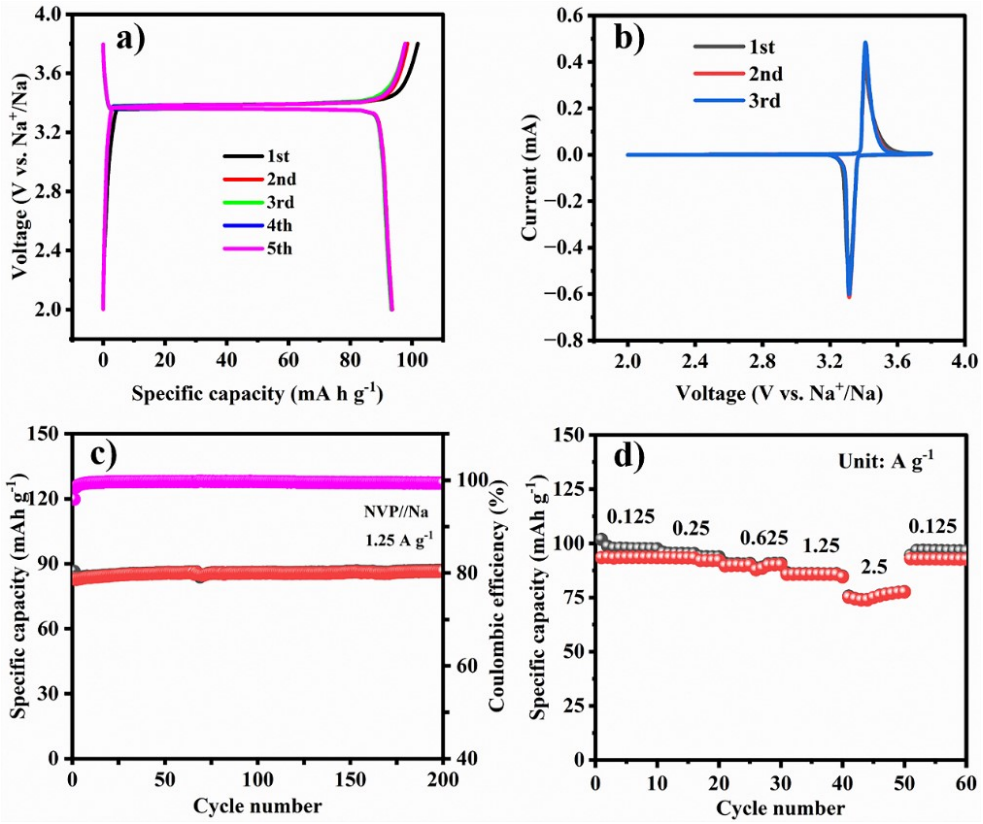

Fig. S25 a) Discharge/charge curve of NVP//Na at 1.25 A g^{-1}, b) first three CV (0.1 mV s^{-1}) curves of NVP//Na. c) electrochemical cycling performance of NVP//Na at 1.25 A g^{-1}, b) rate performance of NVP//Na at different current densities.

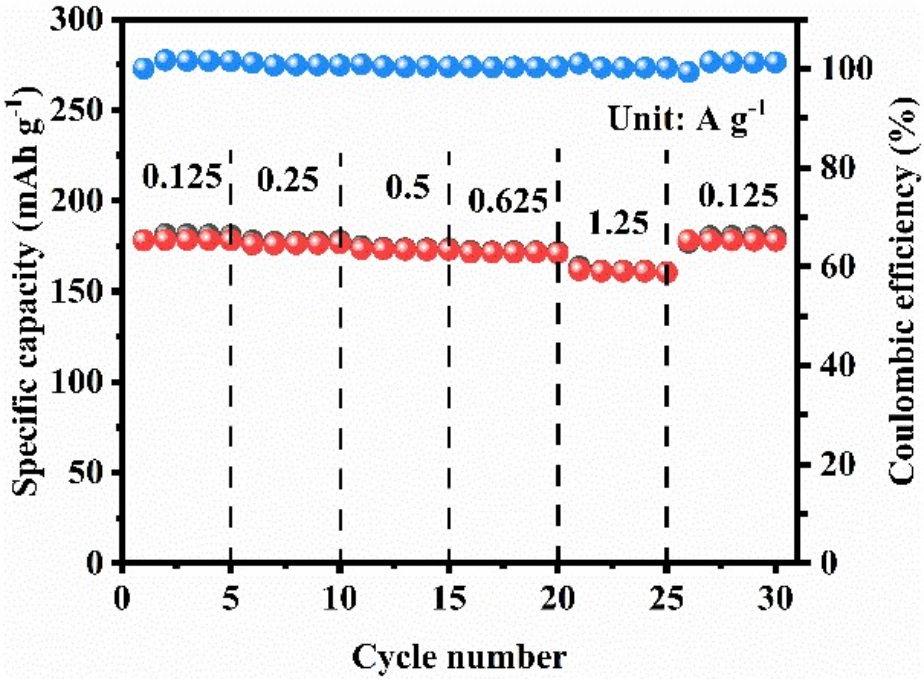

Fig. S26 The rate performance of full cell (NVP | Bi@MC).

Reference

1. Y. Liang, N. Song, Z. Zhang, W. Chen, J. Feng, B. Xi and S. Xiong, *Adv. Mater.*, 2022, **34**, 2202673.
2. Y. H. Kim, J. H. An, S. Y. Kim, X. Li, E. J. Song, J. H. Park, K. Y. Chung, Y. S. Choi, D. O. Scanlon, H. J. Ahn and J. C. Lee, *Adv. Mater.*, 2022, **34**, 2201446.
3. S. Cai, F. Yan, Y. X. Zhao, M. Q. Li, Y. W. Chen, X. R. He and C. Wang, *Chem. Eng. J.*, 2022, **430**, 132938.
4. X. Qiu, X. Wang, Y. He, J. Liang, K. Liang, B. L. Tardy, J. J. Richardson, M. Hu, H. Wu, Y. Zhang, O. J. Rojas, I. Manners and J. Guo, *Sci. Adv.*, 2021, **7**, eabh3482.
5. D. W. Su, S. X. Dou and G. X. Wang, *Nano Energy*, 2015, **12**, 88-95.
6. Y. B. Zhao and A. Manthiram, *Chem. Mater.*, 2015, **27**, 3096-3101.
7. F. H. Yang, F. Yu, Z. A. Zhang, K. Zhang, Y. Q. Lai and J. Li, *Chem. Eur. J.*, 2016, **22**, 2333-2338.
8. S. Liu, J. K. Feng, X. F. Bian, J. Liu and H. Xu, *J. Mater. Chem. A*, 2016, **4**, 10098-10104.
9. C. C. Wang, L. B. Wang, F. J. Li, F. Y. Cheng and J. Chen, *Adv. Mater.*, 2017, **29**, 1702212.
10. J. X. Qiu, S. Li, X. T. Su, Y. Z. Wang, L. Xu, S. Q. Yuan, H. M. Li and S. Q. Zhang, *Chem. Eng. J.*, 2017, **320**, 300-307.

11. S. N. Liu, Z. G. Luo, J. H. Guo, A. Q. Pan, Z. Y. Cai and S. Q. Liang, *Electrochem. Commun.*, 2017, **81**, 10-13.

12. H. Yin, Q. W. Li, M. L. Cao, W. Zhang, H. Zhao, C. Li, K. F. Huo and M. Q. Zhu, *Nano Res.*, 2017, **10**, 2156-2167.

13. L. B. Wang, C. C. Wang, F. J. Li, F. Y. Cheng and J. Chen, *Chem. Commun.*, 2018, **54**, 38-41.

14. J. Chen, X. Fan, X. Ji, T. Gao, S. Hou, X. Zhou, L. Wang, F. Wang, C. Yang, L. Chen and C. Wang, *Energy Environ. Sci.*, 2018, **11**, 1218-1225.

15. J. Xiang, Z. M. Liu and T. Song, *Chemistryselect*, 2018, **3**, 8973-8979.

16. H. Yang, R. Xu, Y. Yao, S. F. Ye, X. F. Zhou and Y. Yu, *Adv. Funct. Mater.*, 2019, **29**, 1809195.

17. X. Cheng, D. Li, Y. Wu, R. Xu and Y. Yu, *J. Mater. Chem. A*, 2019, **7**, 4913-4921.

18. P. Xue, N. Wang, Z. Fang, Z. Lu, X. Xu, L. Wang, Y. Du, X. Ren, Z. Bai, S. Dou and G. Yu, *Nano Lett.*, 2019, **19**, 1998-2004.